Article

Journal of the Brazilian Chemical Society

https://dx.doi.org/10.21577/0103-5053.20240096

J. Braz. Chem. Soc. **2025**, *36*, 1, e-20240096, 1-7

In situ Preparation of Silver Nanoparticles in Polystyrene-*b*-poly(2-vinylpyridine) Films over Chemically Patterned Substrates

Moyra F. Vieira,[a] *Camila G. de Almeida,*[b] *Humberto M. Brandão*[b] *and Celly M. S. Izumi*[*,a]

[a]*Departamento de Química, Instituto de Ciências Exatas, Universidade Federal de Juiz de Fora, Campus Universitário s/n, 36036-900 Juiz de Fora-MG, Brazil*

[b]*Embrapa Gado de Leite, Rua Eugênio do Nascimento, 610, 36038-330 Juiz de Fora-MG, Brazil*

The present work reports the *in situ* fabrication of Ag nanoparticles (AgNPs) in polystyrene-*b*-poly(2-vinylpyridine) (PS-*b*-P2VP) over pre-patterned hydrophobic stripes on a hydrophilic glass surface. Microcontact printing (μCP) using octadecyltrichlorosilane (OTS) as "ink" was used to obtain these chemically modified substrates. A comparison of the results of the PS-*b*-P2VP self-assembly over a bare glass substrate and a pre-patterned glass substrate demonstrated the influence of the pattern on the film morphology. Polymeric films of Ag^+ and PS-*b*-P2VP were prepared on a pre-patterned substrate and heated at 150 °C to enable the self-reconstruction of the polymeric matrix and the *in situ* formation of AgNPs (average particle size of approximately 100 nm). The AgNP/PS-*b*-P2VP thin films were characterized using UV-Vis spectroscopy and atomic force microscopy. The results demonstrate that the concentration of the solutions of Ag^+/PS-*b*-P2VP used to prepare the films strongly influences the morphologies and dispersion of AgNPs. Moreover, the surface-enhanced Raman spectroscopy (SERS) activity of the fabricated polymer nanocomposites using Nile Blue as a molecular probe shows the importance of the chemical modification of the substrate in the enhancement of the SERS signal.

Keywords: block copolymer, nanolithography, polystyrene-*b*-poly(2-vinylpyridine), SERS, silver nanoparticle

Introduction

Metal nanoparticles have been extensively studied because of their optical, electronic, and magnetic properties.[1] Silver nanoparticles (AgNPs) have been used as catalysts, bactericides, and plasmonic material.[2] In addition, AgNPs can sustain localized surface plasmon resonance (LSPR), which is the coherent oscillation of surface-conduction electrons excited by electromagnetic radiation.[3] LSPR excitation induces a strong enhancement in the local magnetic fields close to the surface of the nanoparticles. These regions of strong magnetic fields can be used to intensify the weak signals of molecules adjacent to metallic nanostructures.[4,5] Therefore, AgNPs are suitable for surface-enhanced spectroscopy, such as surface-enhanced Raman scattering (SERS).[4]

In addition, some characteristics of AgNPs, including their dielectric properties, size, shape, and interparticle distance, dictate the LSPR peak extinction wavelength, λ_{max}, and SERS signal.[6] Hence, many methodologies have been developed to synthesize nanoparticles with a variety of sizes and morphologies, such as the chemical reduction of silver ions in aqueous solutions.[2,7] However, these colloids usually exhibit poor stability and aggregate over time.[1] Thus, it is essential to use methods that prevent the aggregation and loss of properties related to the nanometric size.

Self-assembled block copolymers (BCPs) have been extensively studied for many applications in nanotechnology to fabricate efficient, low-cost, large-area periodic nanostructures.[8,9] Amphiphilic BCPs, such as polystyrene-*b*-poly(2-vinylpyridine) (PS-*b*-P2VP), have been extensively used in the *in situ* preparation of metallic nanostructures because of their ability to phase-separate at the nanometer scale. Owing to the unfavorable interactions between the blocks, this phase separation can generate ordered morphologies, such as lamellae, cylinders, and spheres. Consequently, BCPs have been particularly attractive as matrices for metal nanoparticle synthesis, acting as nanoreactors and creating ordered nanoparticle arrays.[10-15]

*e-mail: celly.izumi@ufjf.br
Editor handled this article: Fernando C. Giacomelli (Associate)

Also, the nitrogen atom in the pyridine group of the P2VP block can selectively interact with the metal precursor.[16]

The collective properties of these assemblies, such as the PS-*b*-P2VP molar weight, PS/P2VP ratio, and concentration of the metal precursor, determine the size, morphology, and spatial arrangement of the nanoparticles. Thus, better control over the fabrication of these nanocomposites is essential for future applications of these functional materials.[17,18]

To obtain more complex morphologies, "bottom-up" self-assembly can be combined with "top-down" techniques such as soft lithography.[19] Microcontact printing (μCP) is one of the most explored approaches to microfabrication since it provides the possibility of creating large patterned areas at low cost. In this method, an elastomeric stamp, usually polydimethylsiloxane (PDMS), is used to transfer solutions, "ink," to specific areas of the surface of the substrate.[17,18,20] Mukherjee *et al.*[21] reported the use of metal foils extracted from commercially available data storage discs, such as compact discs (CDs) and digital versatile discs (DVDs), as stamps for surface patterning at low cost and room temperature without applying external pressure. In addition, previous studies[22,23] have demonstrated the use of pre-patterned substrates to guide the self-assembly of polymer thin films. Moreover, Harirchian-Saei *et al.*[24] demonstrated a strategy to directly organize NPs in polystyrene/poly(methyl methacrylate) thin films spin-coated on pre-patterned glass substrates consisting of μCP stripes of octadecyltrichlorosilane (OTS) in a hydrophilic glass substrate using CDs as masters.

In the present study, we combined BCPs self-assembly with microcontact-printed substrates to prepare AgNPs on PS-*b*-P2VP films. Thin films of PS-*b*-P2VP containing Ag^+ ions (Ag^+/PS-*b*-P2VP) were fabricated on glass substrates and AgNPs were produced by thermal *in situ* silver reduction. Microcontact-printed (μCP) patterned glass substrates were used to investigate the effect of surface substrate modification on the morphology of AgNPs/PS-*b*-P2VP films. The SERS activity of the polymer nanocomposites was also studied using Nile Blue as molecular probe.

Experimental

Chemicals

Polystyrene-*block*-poly(2-vinylpyridine) (PS_{389}-*b*-$P2VP_{381}$ with the following number average molecular weights (Mn): $Mn_{(PS)} = 40500\ g\ mol^{-1}$ $Mn_{(P2VP)} = 40000\ g\ mol^{-1}$; and polydispersity (Mw/Mn) of 1.10) was purchased from Polymer Source, Inc (Quebec, Canada). Silver nitrate, octadecyltrichlorosilane (OTS), Sylgard® 184 (PDMS), Nile Blue dye, and all solvents were purchased from Sigma-Aldrich, St. Louis, USA. All reagents were used without further purification.

Microcontact-printed (μCP) patterned glass substrates

μCP patterned glass substrates were prepared by adapting a procedure previously described in the literature.[24]

Therefore, CDs were used as masters to create the patterned PDMS stamps. After removing the protective layer of the CD, the master was cleaned with a water/ethanol solution (1:1) in an ultrasonic bath for 10 min and thoroughly rinsed with deionized water. The PDMS prepolymer and curing agent were mixed in a ratio of 10:1, poured into a Teflon mold placed over the CD polycarbonate master, and cured for 1.5 h at 120 °C. The patterned PDMS stamps were cautiously removed and sonicated in an ethanol/deionized water solution (1:2). A non-patterned flat PDMS stamp was used as an "inkpad", following the previous procedure.

The glass substrates (2 cm × 2 cm) were cleaned in an ultrasonic bath with ethanol, isopropyl alcohol, and acetone for 10 min each. Afterward, the substrates were immersed in piranha solution for 30 min, rinsed thoroughly with deionized water, and dried under ambient conditions to create a hydrophilic layer on the glass. Two drops of the ink solution (OTS in hexane 5 mmol L^{-1}) were spin-coated onto the flat PDMS pad at 3000 rpm for 30 s, which was brought into contact with the patterned PDMS stamp for 60 s. The hydrophobic periodic patterns were transferred to a hydrophilic substrate by placing the inked PDMS stamp over the glass surface for 60 s (Figure 1).

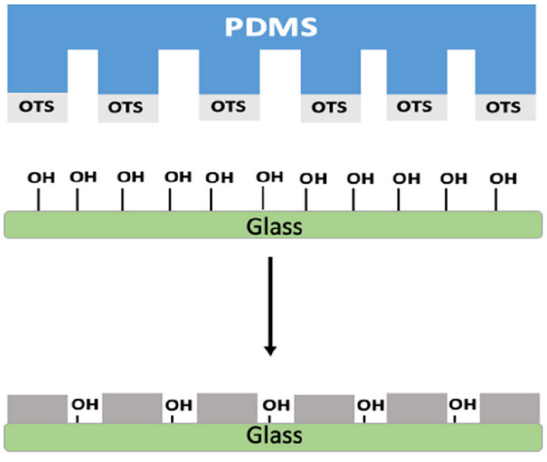

Figure 1. Schematic representation of the μCP process.

The atomic force microscopy (AFM) topographical image and the height profile of the patterned glass

substrates (Figure 2a) show the selective transfer of the OTS to the areas of contact between the PDMS stamp and the hydrophilic substrate by the formation of a bond between the silane and the hydroxyl groups. The resulting substrate presents hydrophobic stripes on a hydrophilic surface. The mean OTS stripes height is 0.873 ± 0.059 nm (Figure 2b), consistent with a flattened OTS monolayer, but still covalently bound to the substrate.[25] These patterned glass substrates were used to direct the organization of spin-coated PS-*b*-P2VP and AgNP/PS-*b*-P2VP films.

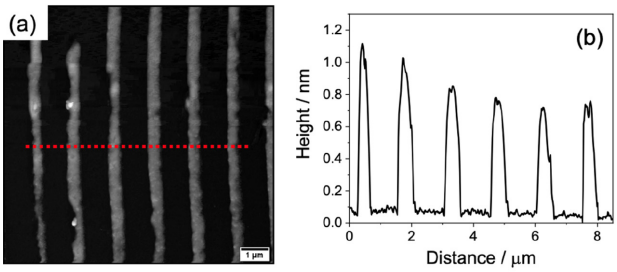

Figure 2. (a) AFM image of µCP OTS patterned glass substrates and (b) height profile along the dashed line.

Preparation of PS-*b*-P2VP and AgNP/PS-*b*-P2VP films

PS_{389}-*b*-$P2VP_{381}$ was dissolved in toluene to obtain a 0.5 wt.% solution, which was stirred for 12 h at room temperature. This 0.5 wt.% solution was diluted to prepare the PS_{389}-*b*-$P2VP_{381}$ solution (0.05 wt.%). Ag^+/PS-b-P2VP solutions were prepared by adding $AgNO_3$ to the PS_{389}-*b*-$P2VP_{381}$ solution in a 1:1 Ag/P2VP molar ratio, followed by vigorous stirring for 12 h at room temperature.

PS-*b*-P2VP films were prepared by spin-coating the polymer solution onto bare glass substrates or µCP patterned glass substrates at 3000 rpm for 60 s.

For *in situ* fabrication of AgNP on PS-*b*-P2VP (AgNP/PS-*b*-P2VP), the Ag^+/PS-*b*-P2VP mixture was spin-coated over bare glass substrates or µCP patterned glass substrates at 3000 rpm for 30 s. The films were then annealed at 150 °C for 1.5 h.

Characterization

UV-Vis absorption spectra were obtained using a Shimadzu UV-1800 spectrophotometer (Juiz de Fora, Brazil) using a quartz cell with a 1.0 cm path length. The thin films on the modified glass substrates were fixed into the sample holder, and a clean glass slide of the same dimensions was used as a reference. The spectra were recorded in the 340-1100 nm range at 0.2 nm resolution.

Raman spectra were obtained using a Bruker SENTERRA spectrometer (Juiz de Fora, Brazil) and a He/Ne laser operating at 633 nm with a maximum power of 2 mW. For the SERS experiments, one drop of Nile Blue solution (1×10^{-4} mol L^{-1}) was added to the AgNP/PS-*b*-P2VP thin film. The films were then washed extensively with deionized water to remove excess dye and dried under vacuum. SERS mappings were performed in 50 µm × 50 µm area, 100 spectra were collected for each sample.

A Nanosurf-Naio AFM (LNNano/CNPEM, Campinas, Brazil) and a Nanosurf Easyscan 2 (Embrapa Gado de Leite, Juiz de Fora, Brazil) AFM in tapping mode with standard AFM cantilevers (Tap190Al-G, R.F. 190 kHz and F.C. 48 N m^{-1}, BudgetSensors) were used to characterize the PS-*b*-P2VP thin film morphologies. Images were post-processed with the SPM software Gwyddion.[26]

The thickness of the PS-*b*-P2VP films was analyzed using a profilometer (KLA, Tencor D-100, Juiz de Fora, Brazil). The average thickness obtained was 10.2 ± 0.8 nm.[27]

Results and Discussion

PS-*b*-P2VP films on glass substrates

A PS-*b*-P2VP solution in toluene was spin-coated onto glass substrates to produce BCP films. Because toluene is a better solvent for PS than P2VP, micelles composed of a core of P2VP and a PS corona are present in this solution.[28] The topographical image of the film produced over an unpatterned glass (Figure 3a) presents a uniform, densely packed micelle morphology. On the other hand, a monolayer of micelles was observed on the surface of the µCP patterned glass substrate (Figure 3b). This result confirms that the polymer and the µCP patterned substrate interactions influence the final film morphology. However, it is not possible to observe stripes due to the high concentration of the Ag^+/PS-*b*-P2VP solution.

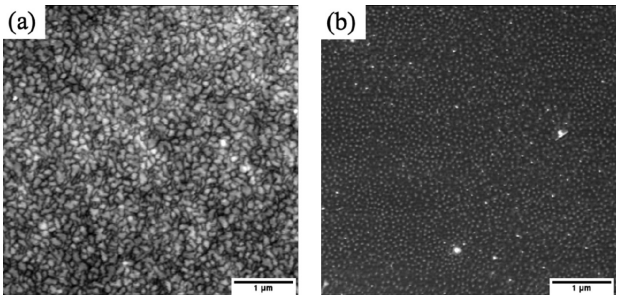

Figure 3. AFM images of PS-*b*-P2VP films on (a) unpatterned glass substrate and (b) µCP glass substrate.

In situ synthesis of AgNP in PS-*b*-P2VP thin film on µCP glass substrate

The formation of reverse micelles of amphiphilic BPC dissolved in a non-polar solvent is well-known;

thereby, when the metal precursor was added to the BCPs solutions, there was a diffusion of the Ag^+ ions to the core of the micelles, where the lone pair of the nitrogen in the P2VP coordinates to the Ag^+ ion creating Ag^+/PS-*b*-P2VP micelle complexes.[29,30] The Ag^+/PS-*b*-P2VP solution was spin-coated on a μCP glass substrate, and the AFM image of this film is shown in Figure 4a. The film consists of a layer of micelles loaded with Ag^+ ions covering the glass surface.

The Ag^+/PS-*b*-P2VP films were annealed at 150 ºC, above the glass transition temperature (Tg) of both blocks.[31,32] This procedure allows polymer self-reconstruction and the reduction of Ag^+ ions to Ag^0 by the nitrogen in the P2VP chains, resulting in AgNP/PS-*b*-P2VP films.[33,34] The AFM topographical image of the AgNP/PS-*b*-P2VP film on the μCP glass substrate is shown in Figure 4b. After thermal annealing of the Ag^+/PS-*b*-P2VP film, large agglomerates of AgNPs (mean diameter = 360 nm) over a porous layer of BCP can be observed. These large agglomerates of AgNPs may be attributed to the high concentration of Ag^+/PS-*b*-P2VP solution.

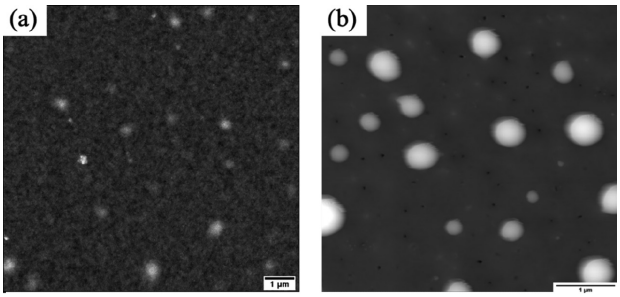

Figure 4. AFM images of (a) Ag^+/PS-*b*-P2VP and (b) AgNP/PS-*b*-P2VP films on μCP glass substrates. Films were produced using a solution of 0.5 wt.% of Ag^+/PS-*b*-P2VP in toluene.

The UV-Vis extinction spectrum of the AgNPs in the PS-*b*-P2VP thin film is shown in Figure 5. A characteristic extinction band from the LSPR of AgNPs is observed at 432 nm, confirming *in situ* synthesis by thermal annealing.

Figure 6a shows the AFM image of Ag^+/PS-*b*-P2VP films prepared from a 0.05 wt.% Ag^+/PS-*b*-P2VP solution before heating; the Ag^+/PS-*b*-P2VP reverse micelles are preferentially adsorbed onto the hydrophobic stripes due to the interaction between the PS chain and the OTS. After thermal annealing, the AFM topographical image of AgNP/PS-*b*-P2VP (Figure 6b) shows the formation of multifaceted AgNPs with an average particle size of approximately 100 nm, well distributed over a porous PS-*b*-P2VP film.

The UV-Vis extinction spectrum of AgNP/PS-*b*-P2VP presents a band with λ_{max} at 437 nm related to isolated AgNPs particles with a narrow size distribution (Figure 7).

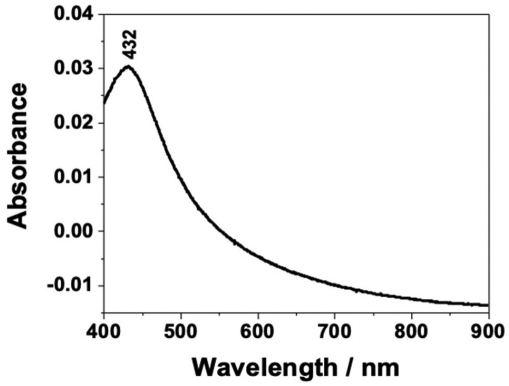

Figure 5. UV-Vis spectrum of AgNP/PS-b-P2VP 0.5 wt.%.

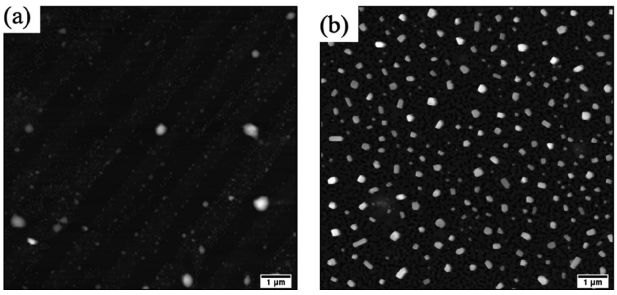

Figure 6. AFM topographical images of (a) Ag^+/PS-*b*-P2VP film and (b) AgNP/PS-*b*-P2VP. Films were produced using a solution of 0.05 wt.% of Ag^+/PS-*b*-P2VP in toluene.

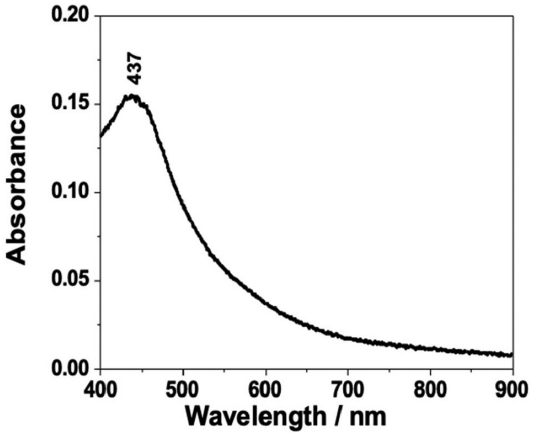

Figure 7. UV-Vis spectrum of AgNP/PS-*b*-P2VP produced using a solution of 0.05 wt.% of Ag^+/PS-*b*-P2VP in toluene.

These results indicate that the concentration of the Ag^+/PS-*b*-P2VP solution strongly influences the size, shape, and organization of AgNPs.

The UV-Vis extinction spectra of the AgNP/PS-*b*-P2VP thin films on non-patterned substrates are shown in the Supplementary Information (SI) section, Figure S1. No distinct extinction band from LSPR was observed at any concentration used. Therefore, it can be concluded that the pre-patterned substrate is essential for the self-organization of PS-*b*-P2VP and, consequently, for the *in situ* synthesis of AgNPs.

SERRS (surface-enhanced resonance Raman spectroscopy)

The SERS activity of the AgNP/PS-*b*-P2VP films (produced from 0.5 or 0.05 wt.% of Ag^+/PS-*b*-P2VP) was evaluated using Nile Blue dye as a molecular probe.

Resonance Raman scattering occurs when the excitation radiation is close to the energy of an electronic transition of the sample, leading to enhanced Raman scattering.[35] In this work, the laser line used as excitation radiation (633 nm) matches the absorption band of chromophoric groups of Nile Blue (Figure S2, SI section).[36,37] The resonance Raman spectrum of the Nile Blue solution (1×10^{-4} mol L^{-1}) is shown in Figure S3 (SI section). Unfortunately, it is not possible to observe any of the Nile Blue characteristic Raman bands due to the fluorescence background that overshadows the Raman bands of the dye. When Nile Blue is adsorbed on an active SERS substrate, the resonance Raman effect is also present, leading to a huge increase of Raman scattering, called SERRS (surface-enhanced resonance Raman scattering).[38]

The mean SERRS spectra of Nile Blue on AgNP/PS-*b*-P2VP (0.5 and 0.05 wt.%) films are shown in Figure S4 (SI section). There is a considerable improvement in the signal-to-noise ratio, background fluorescence quenching, and Raman intensity in those spectra (compared to the resonance Raman of the dye in Figure S3). This result indicates that these films are suitable as SERS substrates.

Figure 8 shows the SERRS maps of AgNP/PS-*b*-P2VP films, monitoring the intensity of Nile Blue's band at 591 cm^{-1}. It is possible to observe that the AgNP/PS-*b*-P2VP (0.5 wt.%) film (Figure 8a) presents weaker SERRS enhancement when compared to AgNP/PS-*b*-P2VP (0.05 wt.%) film (Figure 8b). This result is expected since AgNP/PS-*b*-P2VP (0.5 wt.%) film shows large Ag aggregates unsuitable for enhancing the Raman scattering. Moreover, as the SERS effect amplifies the Raman signal by several orders of magnitude,[39] it is possible to conclude that the Raman signal throughout the analyzed regions is very homogeneous. Moreover, the SERRS map of AgNP/PS-*b*-P2VP (0.05 wt.%) film (Figure 8b) presents

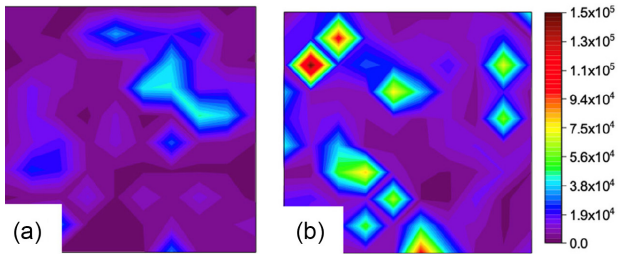

Figure 8. SERRS mapping (50 μm × 50 μm) of the Nile Blue band at 591 cm^{-1}: (a) AgNP/PS-*b*-P2VP (0.5 wt.%) and (b) AgNP/PS-*b*-P2VP (0.05 wt.%).

areas with a high enhancement of Raman signal. This enhancement of the signal may be due to well-distributed multifaceted AgNPs separated by nanoscale gaps, creating regions of high intensification of the electromagnetic field, called hot spots, ideal for enhancing the Raman signal.[40-42]

It is well established that the efficiency of a SERS substrate strongly depends on the characteristics of the nanoparticle, meaning that minor variations in their arrangement can lead to large fluctuations in the SERS signal.[43] Therefore, the methodology described here allows better control over the fabrication of the nanostructures with homogeneous SERRS signals over a large area.

The mean spectra and SERRS mapping of the AgNP/PS-*b*-P2VP (0.5 and 0.05 wt.%) over non-patterned substrates show an intense background fluoresce and very weak SERS signal of the dye (Figure S5, SI section). This result, once more, confirms the importance of the prepatterned substrate for the *in situ* synthesis of AgNPs.

Conclusions

We have demonstrated the *in situ* preparation of AgNPs in PS-*b*-P2VP films and their evaluation as SERS substrates. The use of μCP patterned glass substrates with OTS results in PS-*b*-P2VP films of a uniform monolayer of BCP micelles, essential for the *in situ* synthesis of AgNPs by thermal annealing. We showed that the concentration of Ag^+/PS-*b*-P2VP solution strongly influences the size and aggregation of the AgNPs and the SERRS signal. A PS-*b*-P2VP film with well-distributed multifaceted AgNPs with ca. 100 nm was produced using a 0.05 wt.% of Ag^+/PS-*b*-P2VP solution. Moreover, this film, with uniformly distributed AgNPs and a homogeneous SERRS signal, is a potential material to design SERS substrates for application in sensing. Finally, the methodology outlined here could be adapted for the synthesis of a wide variety of metal nanoparticles (e.g., Pd, Cu, Au) depending on the desired application.

Supplementary Information

Supplementary information is available free of charge at http://jbcs.sbq.org.br as PDF file.

Acknowledgments

This research used facilities of the Brazilian Nanotechnology National Laboratory (LNNano), part of the Brazilian Centre for Research in Energy and Materials (CNPEM), a private non-profit organization under the supervision of the Brazilian Ministry for Science, Technology,

and Innovations (MCTI). The atomic force microscopy staff are acknowledged for their assistance during the experiments (AFM-27489). We acknowledge Dr Cristiano Legnani, Dr Rodrigo Alves Dias and MSc Nayton Claudinei Vicentini for film thickness measurements. This study was financed in part by the Coordenação de Aperfeiçoamento de Pessoal de Nível Superior - Brasil (CAPES) - Finance Code 001 and Fundação de Amparo à Pesquisa do Estado de Minas Gerais (FAPEMIG).

Author Contributions

All the authors contributed to the conception and design of the study. Moyra F. Vieira and Celly M. S. Izumi performed material preparation and analysis. Moyra Freitas Vieira, Camila G. de Almeida, and Humberto M. Brandão performed the data collection. Moyra F. Vieira and Celly M. S. Izumi wrote the first draft of this manuscript. All authors have commented on the previous versions of the manuscript. All the authors have read and approved the final manuscript.

References

1. Goesmann, H.; Feldmann, C.; *Angew. Chem., Int. Ed.* **2010**, *49*, 1362. [Crossref]
2. Dawadi, S.; Katuwal, S.; Gupta, A.; Lamichhane, U.; Thapa, R.; Jaisi, S.; Lamichhane, G.; Bhattarai, D. P.; Parajuli, N.; *J. Nanomater.* **2021**, *2021*, ID 6687290. [Crossref]
3. Willets, K. A.; Van Duyne, R. P.; *Annu. Rev. Phys. Chem.* **2007**, *58*, 267. [Crossref]
4. Malinsky, M. D.; Kelly, K. L.; Schatz, G. C.; Van Duyne, R. P.; *J. Am. Chem. Soc.* **2001**, *123*, 1471. [Crossref]
5. Jeon, T. Y.; Kim, D. J.; Park, S. G.; Kim, S. H.; Kim, D. H.; *Nano Convergence* **2016**, *3*, 18. [Crossref]
6. Kelly, K. L.; Coronado, E.; Zhao, L. L.; Schatz, G. C.; *J. Phys. Chem. B* **2003**, *107*, 668. [Crossref]
7. Khodashenas, B.; Ghorbani, H. R.; *Arabian J. Chem.* **2019**, *12*, 1823. [Crossref]
8. Bates, F. S.; Fredrickson, G. H.; *Phys. Today* **1999**, *52*, 32. [Crossref]
9. Albert, J. N. L.; Epps, T. H.; *Materials Today* **2010**, *13*, 24. [Crossref]
10. Kästle, G.; Boyen, H.-G.; Weigl, F.; Lengl, G.; Herzog, T.; Ziemann, P.; Riethmüller, S.; Mayer, O.; Hartmann, C.; Spatz, J. P.; Möller, M.; Ozawa, M.; Banhart, F.; Garnier, M. G.; Oelhafen, P.; *Adv. Funct. Mater.* **2003**, *13*, 853. [Crossref]
11. Cho, W. J.; Kim, Y.; Kim, J. K.; *ACS Nano* **2011**, 249. [Crossref]
12. Zhang, J.; Gao, Y.; Alvarez-Puebla, R. A.; Buriak, J. M.; Fenniri, H.; *Adv. Mater.* **2006**, *18*, 3233. [Crossref]
13. Goy-López, S.; Juárez, J.; Cambón, A.; Botana, J.; Pereiro, M.; Baldomir, D.; Taboada, P.; Mosquera, V.; *J. Mater. Chem.* **2010**, *20*, 6808. [Crossref]
14. Lee, J.; Yoo, S.; Shin, M.; Choe, A.; Park, S.; Ko, H.; *J. Mater. Chem. A* **2015**, *3*, 11730. [Crossref]
15. Kim, Y. N.; Kum, J. M.; Lee, H. M.; Cho, S. O.; *J. Nanopart. Res.* **2012**, *14*, 774. [Crossref]
16. Svanda, J.; Gromov, M. V.; Kalachyova, Y.; Postnikov, P. S.; Svorcik, V.; Lyutakov, O.; *J. Nanopart. Res.* **2016**, *18*, 289. [Crossref]
17. Lipomi, D. J.; Martinez, R. V.; Cademartiri, L.; Whitesides, G. M.; *Soft Lithographic Approaches to Nanofabrication*; Elsevier: Amsterdam, 2012.
18. Qin, D.; Xia, Y.; Whitesides, G. M.; *Nat. Protoc.* **2010**, *5*, 491. [Crossref]
19. Mukherjee, R.; Sharma, A.; Patil, G.; Faruqui, D.; Sarathi, P.; Pattader, G.; Pattader, P. S. G.; *Bull. Mater. Sci.* **2008**, *31*, 249. [Crossref]
20. Modaresialam, M.; Chehadi, Z.; Bottein, T.; Abbarchi, M.; Grosso, D.; *Chem. Mater.***2021**, *33*, 5464. [Crossref]
21. Mukherjee, R.; Sharma, A.; Gonuguntla, M.; Patil, G. K.; *J. Nanosci. Nanotechnol.* **2008**, *8*, 3406. [Crossref]
22. Bhandaru, N.; Karim, A.; Mukherjee, R.; *Soft Matter* **2017**, *13*, 4709. [Crossref]
23. Roy, S.; Mukherjee, R.; *ACS Appl. Mater. Interfaces* **2012**, *4*, 5375. [Crossref]
24. Harirchian-Saei, S.; Wang, M. C. P.; Gates, B. D.; Moffitt, M. G.; *Langmuir* **2012**, *28*, 10838. [Crossref]
25. Wang, M.; Liechti, K. M.; Wang, Q.; White, J. M.; *Langmuir* **2005**, *21*, 1848. [Crossref]
26. Nečas, D.; Klapetek, P.; *Cent. Eur. J. Phys.* **2012**, *10*, 181. [Crossref]
27. Moyra Vieira, F.; Gabriela Calisto, C. M.; Izumi, C.; *Appl. Surf. Sci.* **2023**, *612*, 155818. [Crossref]
28. Meiners, J. C.; Quintel-Ritzi, A.; Mlynek, J.; Elbs, H.; Krausch, G.; *Macromolecules* **1997**, *30*, 4945. [Crossref]
29. Cong, Y.; Fu, J.; Zhang, Z.; Cheng, Z.; Xing, R.; Li, J.; Han, Y.; *J Appl. Polym. Sci.* **2006**, *100*, 2737. [Crossref]
30. Kong, H.; Jang, J.; *Chem. Commun.* **2006**, 3010. [Crossref]
31. Winkler, R.; Beena Unni, A.; Tu, W.; Chat, K.; Adrjanowicz, K.; *J. Phys. Chem. B* **2021**, *125*, 5991. [Crossref]
32. Rieger, J.; *J. Therm. Anal.* **1996**, *46*, 965. [Crossref]
33. Porel, S.; Singh, S.; Sree Harsha, S.; Narayana Rao, D.; Radhakrishnan, T.; *Chem. Mater.* **2005**, *17*, 9. [Crossref]
34. Porel, S.; Venkatram, N.; Narayana Rao, D.; Radhakrishnan, T. P.; *J. Nanosci. Nanotechnol.* **2007**, *7*, 1887. [Crossref]
35. Clark, R. J. H.; Dines, T. J.; *Angew. Chem., Int. Ed.* **1986**, *25*, 131. [Crossref]
36. Le Ru, E. C. L.; Meyer, S. A.; Artur, C.; Etchegoin, P. G.; Grand, J.; Lang, P.; Maurel, F.; *Chem. Commun.* **2011**, *47*, 3903. [Crossref]
37. Andrade, G. F. S.; Min, Q.; Gordon, R.; Brolo, A. G.; *J. Phys. Chem. C* **2012**, *116*, 2672. [Crossref]
38. McNay, G.; Eustace, D.; Smith, W. E.; Faulds, K.; Graham, D.; *Appl. Spectrosc.* **2011**, *65*, 825. [Crossref]

39. Le Ru, E. C.; Etchegoin, P. G.; *Principles of Surface-Enhanced Raman Spectroscopy*; Elsevier: Amsterdam, 2009.
40. Piaskowski, J.; Bourret, G. R.; *Molecules* **2022**, *27*, 2485. [Crossref]
41. Moskovits, M.; *J. Raman Spectrosc.* **2005**, *36*, 485. [Crossref]
42. Fan, M.; Andrade, G. F. S.; Brolo, A. G.; *Anal Chim Acta* **2011**, *693*, 7. [Crossref]
43. Fan, M.; Andrade, G. F. S.; Brolo, A. G.; *Anal Chim Acta* **2020**, *1097*, 1. [Crossref]

Submitted: February 26, 2024
Published online: June 6, 2024